Microplate motions in the hotspot reference frame

Marco Cuffaro[1] and Donna M. Jurdy[2]

[1]*Dipartimento di Scienze della Terra, Università degli Studi di Roma "La Sapienza", P.le A. Moro 5, 00185 Rome, Italy;* [2]*Department of Geological Sciences, Northwestern University, 1850 Campus Drive, Evanston, IL 60208, USA*

ABSTRACT

We have computed motions of the major plates (seven large plates and seven medium-sized plates) and 38 microplates relative to the hotspot reference frame, and present velocities of these 52 plates. Moreover, using updated plate boundaries for the present, we have computed new geometrical factors for plates and microplates, useful for kinematic calculations and to obtain the net-rotation of the lithosphere and plate velocities in the mean-lithosphere reference frame. Instead of a continuum or gradational distribution of the plates by size, the plates clearly partition into three groups each having their own characteristics. For the seven large plates, rotation poles generally lie in high latitudes; the seven medium-sized plates have rotation poles in a restricted equatorial area; the 38 small plates show the greatest scatter. Moreover subsets of the 52 plates reveal differing fractal behaviour: the large, middle and small groupings each have a characteristic fractal dimension, suggestive of microplate clustering. The highest angular velocities occur for some of the smallest plates, with the location of their rotation poles closeby.

Terra Nova, 18, 276–281, 2006

Introduction

In this paper, we compute absolute motions that describe the motion of plates and microplates with respect to the mesosphere. In plate kinematic and dynamic analyses, two different absolute reference frames have been utilized: fixed-hotspots and mean-lithosphere. The first, the 'hotspot reference frame', is based on the assumption that individual hotspots are fixed relative to the mesosphere and to each other (Morgan, 1972; Wilson, 1973). Under this hypothesis, a seamount chain such as the Hawaiian-Emperor describes the motion of the overlying Pacific plate relative to the Hawaiian hotspot assumed stationary. The second frame, for the no-net-rotation condition (NNR) (Solomon and Sleep, 1974), rests upon the assumption that lithosphere and asthenosphere are uniformly coupled. Because both absolute reference frames are referred to the mesosphere, any difference between the frames would be interpreted as a net-rotation of the lithosphere with respect to the mesosphere (Forsyth and Uyeda, 1975).

Here, we choose the hotspot reference frame (Gripp and Gordon, 2002) to describe 52 plate and micro-plate motions. In addition, we compute plate and microplate velocities in the corresponding NNR frame.

Methods and results

Gripp and Gordon (2002) defined a hotspot reference frame using 11 segment trends and two volcanic propagation rates, obtaining absolute plate motions for an *c.* 5.8 Myr time interval. First, they estimated segment trends and volcanic propagation rates by least-square methods and then, in this frame, computed a set of angular velocities consistent with the relative plate motions model NUVEL-1A (DeMets *et al.*, 1990, 1994). In their study, only the Hawaiian and Society tracks were used to position the Pacific plate, giving a Pacific angular velocity of $1.0613°$ Myr^{-1} about a pole located at 61.467°S, 90.326°E. Adding the Pacific plate angular velocity to the relative model NUVEL-1A (DeMets *et al.*, 1990, 1994) results in the present-day velocities in the hotspot reference frame.

Using these methods, we computed plate and microplate motions in the hotspot frame, using the PB2002 database (Bird, 2003) for 52 plates (Table 1 and Fig. 1). The PB2002 model also gives 52 new plate boundaries in digital form, and relative plate and microplate motions are referred to an arbitrary Pacific plate fixed, some coming from the literature, others newly interpreted. In that model, the velocities of the 10 largest plates,

Africa (AF), Antarctica (AN), Arabia (AR), Australia (AU), Cocos (CO), Eurasia (EU), India (IN), Nazca (NZ), North America (NA) and South America (SA) come from the NU-VEL-1A (DeMets *et al.*, 1990, 1994); therefore for these plates we exactly reproduced the HS3-NUVEL1A results (Gripp and Gordon, 2002) (Table 1). Using the other relative motions collected and proposed by Bird (2003, his Table 1), we obtain new Euler vectors relative to the hotspots for the remaining 42 plates and microplates (Table 1).

Although the covariance matrix of the Pacific plate is computed by Gripp and Gordon (2002), the uncertainties of the angular velocities for plates and microplates in the hotspots are not presented in this paper, because the errors of relative plate motions of the PB2002 model (Bird, 2003) are not reported. Using errors of 50 km for the location of individual hotspots, Jurdy (1990) calculated an uncertainty of 1.1° for the hotspot reference frame. Thus, in view of that study and also the standard deviations of the HS3-NUVEL1A model (Gripp and Gordon, 2002) for plate Euler vectors, we would obtain rather large uncertainties for microplate angular velocities.

Figure 1 shows current plate and microplate linear velocities relative to the hotspots. Most of the microplates are on the Pacific-Australia boundary (Fig. 1a,b). Their motions are principally W-NW-ward directed with different velocities, except for

Correspondence: Marco Cuffaro, Dipartimento di Scienze della Terra, Università degli Studi di Roma "La Sapienza", P. le A. Moro 5, 00185 Rome, Italy. Tel.: 39 06 4991 4156; fax: 39 06 4454 729; e-mail: marco.cuffaro@uniroma1.it

Table 1 Microplate and plate geometrical factors and angular velocities relative to the hotspots. Plates are sorted by area

| Plate | Definition | Area* | Angular velocity | | | Geometrical factors* | | | | | |
			°N	°E	°Myr^{-1}	I_{xx}	I_{yy}	I_{zz}	I_{xy}	I_{xz}	I_{yz}
PA	Pacific	2.5768	−61.467	90.326	1.0613	1.1757	1.9612	2.0168	−0.4295	0.0774	−0.0574
AF	Africa	1.4407	−43.386	21.136	0.1987	0.3726	1.3012	1.2075	−0.0513	−0.0054	0.0442
AN	Antarctica	1.4326	−47.339	74.514	0.2024	1.3267	1.1747	0.3638	−0.0510	0.0525	0.0813
NA	North America	1.3657	−74.705	13.400	0.3835	1.2286	0.9416	0.5612	0.0662	−0.0036	0.3963
EU	Eurasia	1.1963	−61.901	73.474	0.2047	1.0059	0.8948	0.4919	−0.0356	−0.2132	−0.3103
AU	Australia	1.1329	−0.091	44.482	0.7467	0.8003	0.5884	0.8772	0.2032	−0.2132	0.2881
SA	South America	1.0305	−70.583	80.401	0.4358	0.6255	0.6092	0.8262	0.3403	0.1914	−0.1716
SO	Somalia	0.4719	−53.406	4.344	0.1192	0.2842	0.2349	0.4248	−0.1982	0.0608	0.0655
NZ	Nazca	0.3967	35.879	−90.913	0.3231	0.3854	0.0684	0.3396	−0.0126	−0.0030	−0.1134
IN	India	0.3064	3.069	26.467	0.5211	0.2863	0.0423	0.2841	−0.0570	−0.0131	−0.0605
SU	Sunda	0.2197	−6.772	−26.816	0.2037	0.1888	0.0363	0.2142	0.0691	0.0065	−0.0168
PS	Philippine Sea	0.1341	−52.742	−16.819	1.1978	0.0777	0.0713	0.1192	0.0583	0.0266	−0.0276
AM	Amur	0.1306	−70.123	12.836	0.1553	0.1082	0.0895	0.0636	0.0287	0.0363	−0.0513
AR	Arabia	0.1208	2.951	23.175	0.5083	0.0742	0.0668	0.1006	−0.0488	−0.0296	−0.0310
OK	Okhotsk	0.0748	−74.713	28.719	0.2454	0.0534	0.0664	0.0298	0.0130	0.0303	−0.0179
CA	Caribbean	0.0731	−64.494	−6.969	0.2196	0.0660	0.0120	0.0681	0.0180	−0.0052	0.0171
CO	Cocos	0.0722	13.171	−116.997	1.1621	0.0711	0.0030	0.0704	−0.0055	0.0011	0.0101
YA	Yangtze	0.0543	0.005	108.306	0.1617	0.0457	0.0200	0.0429	0.0166	0.0096	−0.0195
SC	Scotia	0.0419	−77.268	51.747	0.4512	0.0367	0.0345	0.0126	0.0057	0.0120	−0.0145
CL	Caroline	0.0377	−67.826	54.057	0.9482	0.0153	0.0225	0.0375	0.0182	0.0016	−0.0013
ND	North Andes	0.0239	−66.874	88.610	0.3629	0.0224	0.0020	0.0235	0.0058	−0.0007	0.0025
AP	Altiplano	0.0205	−57.402	−65.177	0.5044	0.0182	0.0042	0.0187	0.0061	0.0021	−0.0054
BS	Banda Sea	0.0171	−7.931	116.220	2.5106	0.0113	0.0060	0.0170	0.0088	−0.0009	0.0012
NH	New Hebrides	0.0158	−7.206	−0.892	2.5912	0.0019	0.0154	0.0143	0.0023	−0.0045	0.0008
AT	Anatolia	0.0142	21.319	35.874	1.1875	0.0080	0.0116	0.0088	−0.0040	−0.0058	−0.0037
BH	Birds Head	0.0130	−47.199	89.453	1.181	0.0072	0.0058	0.0129	0.0064	−0.0002	0.0002
BU	Burna	0.0127	−13.616	−72.199	2.2091	0.0126	0.0004	0.0123	0.0009	0.0001	−0.0019
KE	Kermadec	0.0124	30.673	11.939	2.2652	0.0038	0.0124	0.0087	−0.0001	−0.0056	0.0000
WL	Woodlark	0.0112	−10.765	121.708	1.8733	0.0035	0.0078	0.0110	0.0050	−0.0011	0.0007
MA	Mariana	0.0104	−2.188	129.087	1.2627	0.0040	0.0074	0.0094	0.0044	0.0025	−0.0017
MS	Molucca Sea	0.0103	−2.378	−52.330	3.582	0.0072	0.0031	0.0103	0.0047	−0.0001	0.0002
NB	North Bismarck	0.0096	−51.303	109.171	1.2242	0.0026	0.0070	0.0095	0.0042	−0.0004	0.0002
TI	Timor	0.0087	−12.605	106.497	1.9539	0.0058	0.0031	0.0085	0.0040	−0.0008	0.0011
ON	Okinawa	0.0080	28.131	132.145	2.5439	0.0056	0.0041	0.0063	0.0030	0.0020	−0.0026
AS	Aegean Sea	0.0080	−42.838	89.030	0.4515	0.0038	0.0070	0.0051	−0.0019	−0.0034	−0.0016
SB	South Bismarck	0.0077	4.427	−29.965	8.0525	0.0021	0.0056	0.0076	0.0033	−0.0006	0.0003
PM	Panama	0.0068	−82.553	−101.535	0.1998	0.0066	0.0003	0.0066	0.0001	−0.0002	0.0010
JF	Juan De Fuca	0.0064	−39.368	61.745	1.0117	0.0052	0.0044	0.0031	−0.0015	0.0019	0.0025
TO	Tonga	0.0063	23.449	5.813	8.9185	0.0008	0.0062	0.0055	−0.0005	−0.0019	−0.0002
BR	Balmoral Reef	0.0049	−64.237	97.967	0.8758	0.0004	0.0048	0.0045	0.0003	−0.0012	0.0001
SW	Sandwich	0.0046	−46.255	−24.275	2.1207	0.0035	0.0043	0.0013	0.0005	0.0018	−0.0009
EA	Easter	0.0042	23.065	67.522	11.4154	0.0036	0.0013	0.0034	−0.0013	−0.0006	−0.0014
CR	Caonway Reef	0.0036	−25.548	167.064	3.9894	0.0004	0.0035	0.0032	0.0003	−0.0011	0.0001
SS	Solomon Sea	0.0032	−13.765	123.523	1.8422	0.0007	0.0025	0.0031	0.0013	−0.0004	0.0002
NI	Niuafo'ou	0.0031	−9.705	182.111	3.222	0.0003	0.0030	0.0028	−0.0002	−0.0008	−0.0001
MO	Maoke	0.0029	−9.667	84.933	0.9678	0.0013	0.0016	0.0028	0.0014	−0.0001	0.0001
RI	Riviera	0.0025	17.605	−107.298	3.8881	0.0023	0.0005	0.0022	−0.0006	0.0002	0.0008
JZ	Juan Fernandez	0.0024	33.26	70.701	22.3832	0.0022	0.0009	0.0017	−0.0006	−0.0004	−0.0010
SL	Sherland	0.0018	−51.811	112.365	0.2151	0.0017	0.0015	0.0004	0.0002	0.0004	−0.0006
FT	Futuna	0.0008	−20.476	175.617	5.1096	0.0001	0.0008	0.0007	0.0000	−0.0002	0.0000
GP	Galapagos	0.0003	−0.713	77.892	5.6985	0.0003	0.0000	0.0004	−0.0001	0.0000	0.0000
MN	Manus	0.0002	−4.056	149.967	51.6116	0.0000	0.0002	0.0002	0.0001	0.0000	0.0000
LS	Lithosphere	12.566	−55.319	69.384	0.4296	8.3777	8.3777	8.3778	0.0002	−0.0002	0.0004

*Units are in steradians.

the Niuafo'ou (NI), Kermadec (KE) and Tonga (TO) microplates (E-NE-ward directed) (Fig. 1b). The other small plate velocities are generally W-NW-ward oriented except for the Sandwich (SW) and Galapagos (GP) microplate (Fig. 1c) (SW-ward oriented). Easter Island (EA) and Jun Fernandez (JZ) show a NW-ward
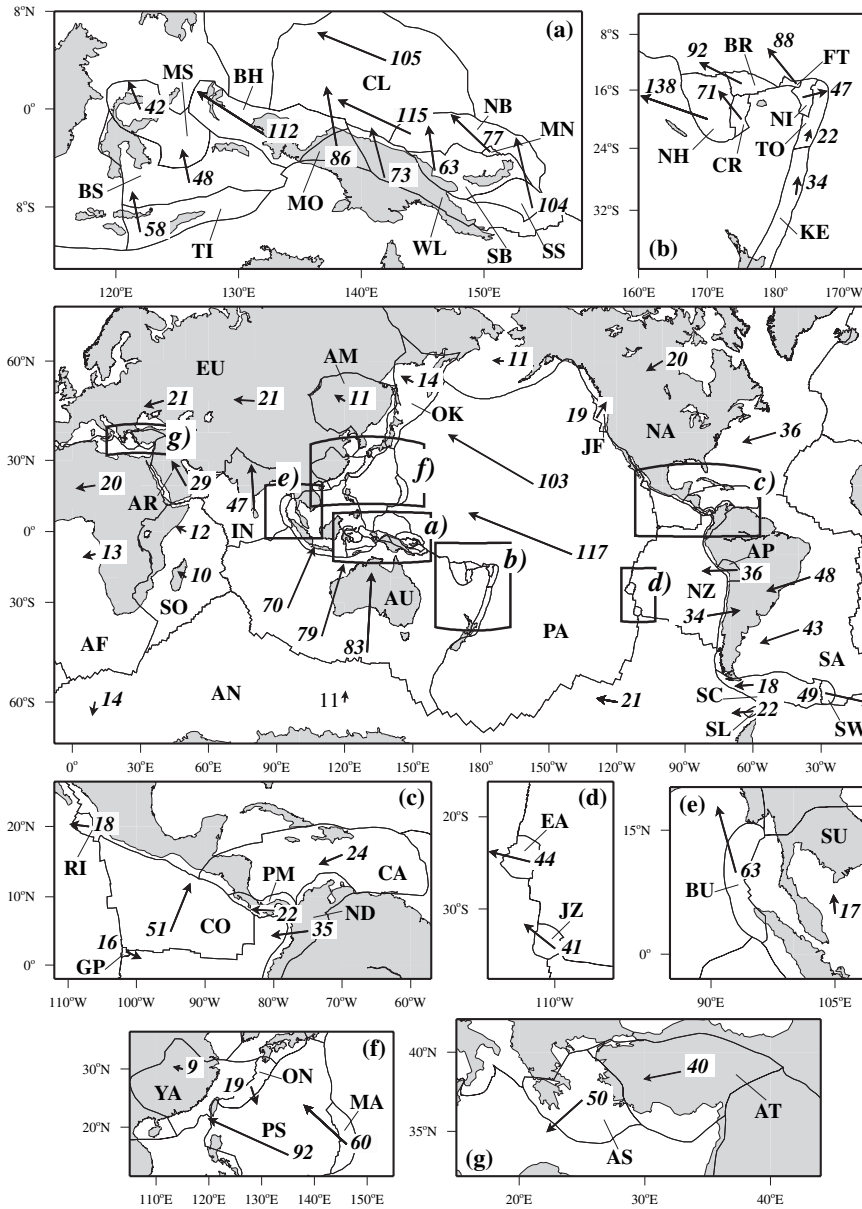
Fig. 1 Microplate and plate motions with respect to the hotspot reference frame. Units are in mm yr^{-1}.

direction (Fig. 1d), whereas Burna (BU) (Fig. 1e) is mostly N-ward directed and Okinawa (ON) (Fig. 1f) is SE-ward directed. Egean Sea (AS) and Anatolia (AT) (Fig. 1g) have instead SW-ward oriented linear velocities.

Starting with these data, we compute plate and microplate geometrical factors, useful to compute net-rotation of the lithosphere. We define the symmetric tensor I_p (Gordon and Jurdy, 1986; Jurdy, 1990) describing plate geometry for a single plate p on a unit sphere:

$$I_p = \int_S \begin{bmatrix} 1-x^2 & -xy & -xz \\ -xy & 1-y^2 & -yz \\ -xz & -yz & 1-z^2 \end{bmatrix} dS \quad (1)$$

where x, y, z are the Cartesian coordinates of a plate p, S the plate surface and dS is the area element. The x-, y- and z-directions are defined from the centre of the Earth to (0°N, 0°E), (0°N, 90°E) and (90°N, 0°E), respectively. Geometrical factors of plates and microplates defined by Eq. (1) are reported in Table 1.

The net-rotation of the lithosphere concept can assume different geo-

physical meanings (Lliboutry, 1974; Solomon and Sleep, 1974); it also describes the NNR framework rotation with respect to the hotspot frame (Argus and Gordon, 1991).

The net-rotation angular velocity ω_{nr} can be computed with a matrix equation:

$$\omega_{nr} = \frac{3}{8\pi} \sum_{p=1}^{P} I_p \omega_p \quad (2)$$

where P is the total number of plates and microplates, I_p is geometrical factors for plate p, and ω_p is the

angular velocity for that plate (Table 1).

The resulting present net-rotation of the lithosphere relative to the mesosphere is described by a right-handed rotation about an Euler pole at 55.319°S, 69.384°E and 0.4296° Myr^{-1}.

To obtain the angular velocity of a single plate p in the mean-lithosphere frame, the net-rotation angular velocity ω_{nr} is subtracted from the angular velocity ω_p. The mean-lithosphere framework is a reference frame based on the global plate geometry and velocities of every plate. Thus, any change in the assumed relative plate velocities and geometry results in a different net-rotation of the lithosphere. Indeed, using various plate motion models, hotspot locations or geometrical factors yield different values of net-rotation angular velocity: 0.251° Myr^{-1} about a pole located at 51.50°S, 65.60°E (Harper, 1986); 0.150° Myr^{-1} about a pole located at 56.00°S, 84.00°E (Ricard et al., 1991); 0.33° Myr^{-1} about a pole located at 49.20°S, 64.90°E (Argus and Gordon, 1991); 0.436° Myr^{-1} about a pole located at 55.91°S, 69.93°E (Gripp and Gordon, 2002). Although unresolved questions about hotspots remain, such as the number and the source depth (Foulger et al., 2005), nonetheless the hotspot reference frame remains a convenient – and easy to visualize – framework in which to study plate kinematics and dynamics. Thus we utilize the hotspot framework in our study.

Discussion

We have estimated current velocities for the plates including 38 new microplates in the hotspot reference frame, incorporating the PB2002 model (Bird, 2003). We also present a new net-rotation angular velocity including microplate contributions and necessary rotation to obtain plate angular velocities in the mean-lithosphere framework. Our results (Table 1, Figs 2–5) show some kinematic and geometric patterns related to plate size. No continuum or gradational distribution of plate size exists. Plates clearly partition into three groups: large, middle and small. The seven large plates (PA, AF, AN, NA, EU, AU, SA) all exceed 1.03 sr;

together these comprise 81.0% of the Earth's surface and dominate with 85.3% of the net-rotation velocity computation. Next, the seven middle plates (SO, NZ, IN, SU, PS, AM, AR), in the range of 0.47–0.12 sr, cover 14.0% of the surface area and contribute 9.8% of the velocity computation. The remaining 38 plates span three orders of magnitude in size and lie in the range 0.0748–0.0002 sr, accounting for 4.9% of the total area and 5.2% of the total net-rotation.

The distribution of the plates over Earth's surface shows a relation to the size-grouping of plates. The large-sized lithospheric plates cover most of the Earth's surface. Middle-sized plates are positioned in equatorial regions (except AM, Fig. 2), whereas most of the small plates lie on the interfaces of the large plates, i.e. the Australia-Pacific, the Eurasia-Pacific and the Nazca-South America boundary (Fig. 2), suggesting that some might be interpreted as parts of the diffuse margin of the two large plates. In addition, the plate angular velocities show a pattern with plate size: these generally increase with decreasing plate area (Fig. 3) reaching the
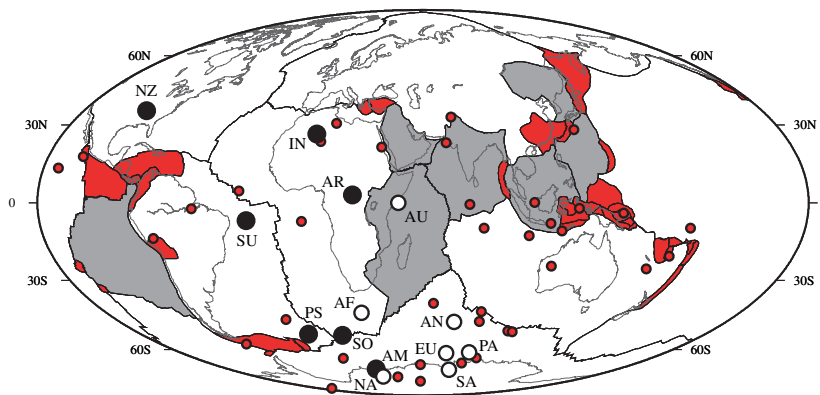

Fig. 2 Large (white), middle (grey) and small (red) plates and respective rotation poles, open, black and red circles.
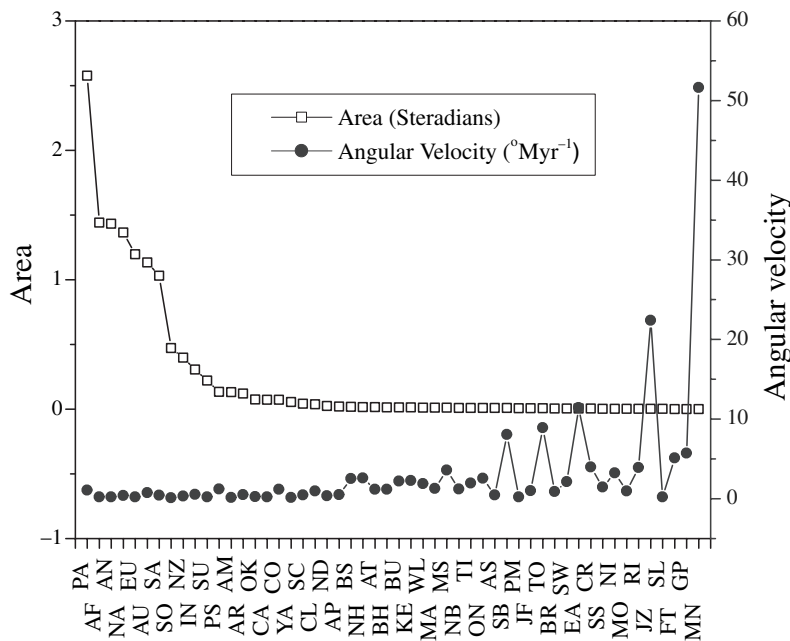

Fig. 3 Microplates and plates (sorted by area) vs. plate area (left axis) and angular velocities relative to the hotspots (right axis).

Microplate motions in the hotspot reference frame • M. Cuffaro and D. M. Jurdy

Terra Nova, Vol 18, No. 4, 276–281
....
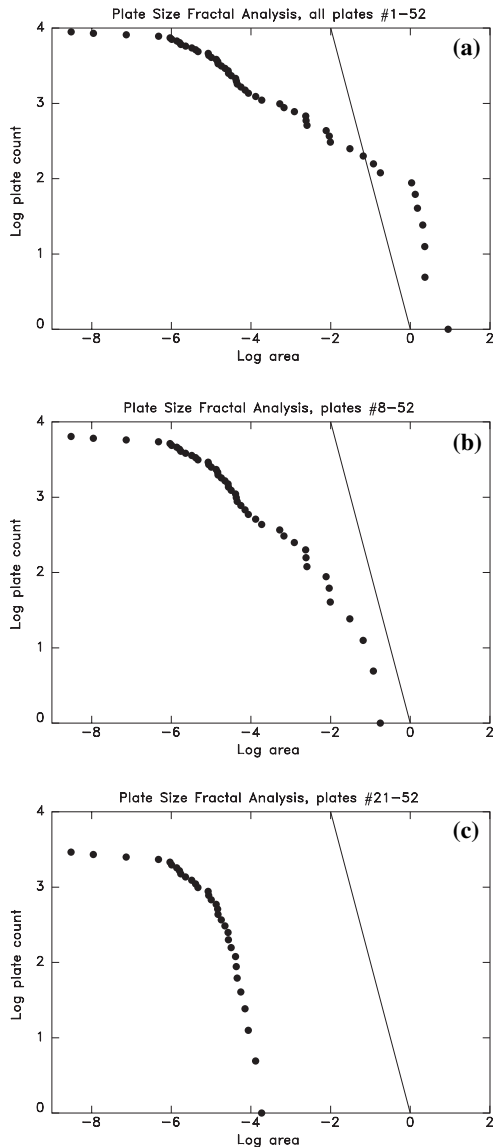
Fig. 4 Log of plate count vs. the log of the plate area in steradians. The 52 plates have non-fractal behaviour. The largest seven plates show one slope (a), wheareas the remaining plates show another, (b) for middle plates, (c) for the remaining microplates. Reference line has a slope of −2.

highest values for some of the smallest plates (e.g. JZ and MN).

Fractals relate geometry at different scales, and as Feder (1988) argues, can give insight into our understanding of naturally occurring objects. The plates, which range in size over four orders of magnitude (Table 1), provide a compelling opportunity for fractal analysis. We examine the fractal behaviour of the plates by plotting the log of the plate area in steradians vs. the log of the plate count (shown in Fig. 4). Bird has considered the fractal properties of the plates (Bird, 2003, his Fig. 19) and finds that the plates having areas between 0.002 and 1.000 sr (JZ to SA for his 38 plates) can be approximately described by a power law:

$$Cc \approx 7A^{-1/3} \qquad (3)$$

where Cc is the cumulative count of plates and A is the plate area in steradians.

Here, we note that the fractal behaviour of the plates also depends on the size range. In Fig. 4, we show that the largest seven plates define one slope, or fractal behaviour, and the middle seven another slope, whereas remaining 38 plates have a different fractal behaviour. The largest seven (omitting the Pacific as an exception, as Bird has done) have a slope of less than −2 (Fig. 4a). The middle-sized plates (Fig. 4b) have a slope of less than −2 (the reference line), and the small plates – particularly no. 22–48 match the reference line slope of −2 (Fig. 4c). The change in slope from −2 may be a consequence of a clustering behaviour for the smaller plates. This clustering ceases once the plate's size increases from about 4% to more than 12% of the surface of the Earth. Feder (1988) shows a similar fractal behaviour for the clustering of silica particles (e.g. Feder, 1988, Chapter 3). The curve flattens for the smallest plates. Bird's explanation for this flattening of the curve lies in the current incompleteness of the data set for plates smaller than SL, 0.0002 sr.

Additional patterns emerge concerning the absolute motions of the plates based on their groupings by size. The Euler poles for large plates concentrate over less than 10% of a hemisphere near a mean latitude of 60°S, except for AU, a consequence of its north-west motion (Fig. 5a). However, the Euler poles for middle-sized plates are generally more equatorial in distribution, but scatter more, spread over about 20% of a hemisphere (Fig. 5a). The rotation poles of the small plates generally show considerable scatter, although poles avoid the regions populated by the poles for the large and middle-sized plates (Fig. 5b). This is a consequence of microplate behaviour, as noted by Engeln et al. (1998): the rotation poles describing microplate motion lie close by, thus have large rotations. This may explain the difference in location of rotation poles and size of the rotation for small microplates, when compared with the seven larger plates. These high velocities and the locations of rotation poles fairly close to the corresponding plates may offer a criterion to distinguish independent microplates from diffuse margins.

We have shown in this paper that there appears to be a natural partitioning of plates into three groups based on their size. Each subset of plates shares some common charac-
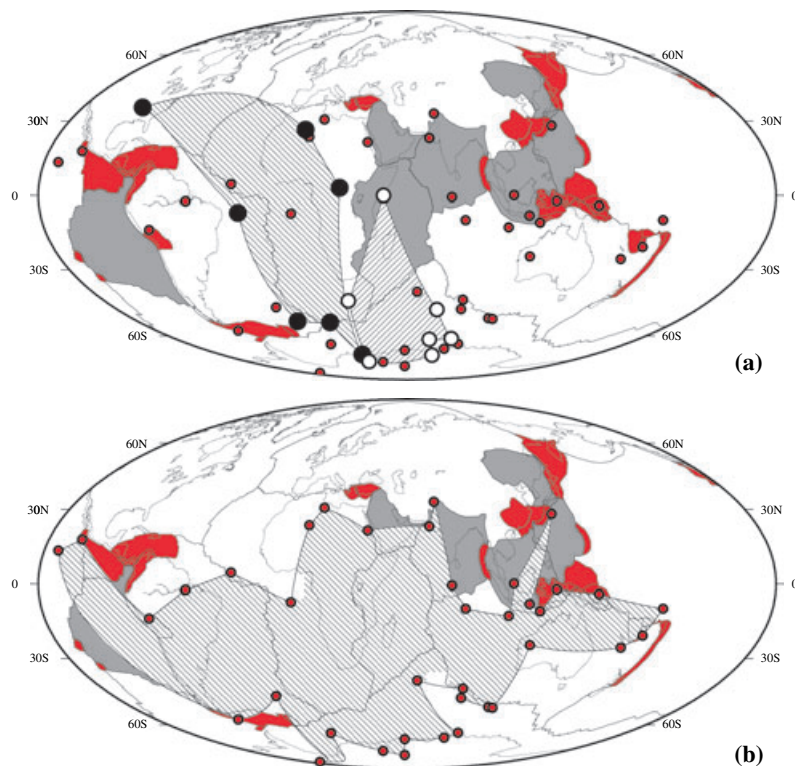
Fig. 5 (a) The Euler poles for large plates concentrate over les that 10% of a hemisphere near a mean latitude of 60°S, except for AU. However, the Euler poles for middle-sized plates are generally more equatorial in distribution, and these scatter more, about 20% of a hemisphere. (b) The rotation poles of the small plates generally show considerable scatter, although poles avoid the regions populated by the poles for the large and most of middle-sized plates.

teristics. These similarities within groups include the nature of plate distribution over the Earth, location of rotation poles, size of the corresponding rotations, as well as the observed fractal behaviour. This breakdown by plate size may be a natural consequence of plate tectonics: large plates and most of the middle being moved predominantly by driving forces, and small ones clustering at the interfaces.

References

Argus, D.F. and Gordon, R.G., 1991. No-net-rotation model of current plate velocities incorporating plate motion model NUVEL-1. *Geophys. Res. Lett.*, **18**, 2039–2042.

Bird, P., 2003. An updated digital model of plate boundaries. *Geochem. Geophys. Geosyst.*, **4**, doi: 10.1029/2001GC000252.

DeMets, C., Gordon, R.G., Argus, D.F. and Stein, S., 1990. Current plate motions. *Geophys. J. Int.*, **101**, 425–478.

DeMets, C., Gordon, R.G., Argus, D.F. and Stein, S., 1994. Effect of recent revisions to the geomagnetic reversal time scale on estimates of current plate motions. *Geophys. Res. Lett.*, **21**, 2121–2194.

Engeln, J.F., Stein, S., Werner, S. and Gordon, R.G., 1998. Microplate and shear zone models for oceanic spreading center reorganizations. *J. Geophys. Res.*, **93**, 2839–2856.

Feder, J., 1988. *Fractals*. Plenum Press, New York.

Forsyth, D.W. and Uyeda, S., 1975. On the relative importance of the driving forces of plate motion. *Geophys. J. Roy. Astron. Soc.*, **43**, 163–200.

Foulger, G.R., Natland, J.H., Presnall, D.C. and Anderson, D.L., 2005. Plates, plumes, and paradigms. *Geol. Soc. Am. Spec. Pap.*, **388**, 861pp.

Gordon, R.G. and Jurdy, D.M., 1986. Cenozoic global plate motions. *J. Geophys. Res.*, **91**, 12384–12406.

Gripp, A.E. and Gordon, R.G., 2002. Young tracks of hotspots and current plate velocities. *Geophys. J. Int.*, **150**, 321–364.

Harper, J.F., 1986. Mantle flow and plate motions. *Geophys. J. Roy. Astron. Soc.*, **87**, 155–171.

Jurdy, D.M., 1990. Reference frames for plate tectonics and uncertainties. *Tectonophysics*, **182**, 373–382.

Lliboutry, L., 1974. Plate movement relative to a rigid lower mantle. *Nature*, **250**, 298–300.

Morgan, W.J., 1972. Plate motions and deep mantle convection. *Studies in Earth and Space Sciences, Geol. Soc. Am. Mem.*, **132**, 7–22.

Ricard, Y., Doglioni, C. and Sabadini, C., 1991. Differential rotation between lithosphere and mantle: a consequence of lateral viscosity variations. *J. Geophys. Res.*, **96**, 8407–8415.

Solomon, S. and Sleep, N.H., 1974. Some simple physical models for absolute plate motions. *J. Geophys. Res.*, **79**, 2557–2567.

Wessel, P. and Smith, W.H.F., 1995. New version of generic mapping tools released. *EOS Trans. Am. Geophys. Union*, **76**, 329.

Wilson, J.T., 1973. Mantle plumes and plate motions. *Tectonophysics*, **19**, 149–164.